A Hemispherical 3-D Null Steering Antenna for Circular Polarization

Changjiang Deng, *Student Member, IEEE*, Yue Li, *Member, IEEE*, Zhijun Zhang, *Fellow, IEEE*, and Zhenghe Feng, *Fellow, IEEE*

***Abstract*—In this letter, a compact three-dimensional (3-D) null steering antenna is presented for circular polarization. Two high-isolated circularly polarized (CP) pattern modes, the broadside and the conical CP pattern modes, are synthesized for 3-D null steering in the upper hemisphere. The broadside CP pattern mode is generated by a corner-truncated patch, and the conical CP pattern mode is generated by four rotationally symmetric strips. By controlling the exciting power ratio and the relative phase delay of the two modes, continuous null steering is achieved in the elevation plane and the azimuth plane, respectively. A prototype of the proposed antenna operating at 1.575 GHz is fabricated and tested for the global position system (GPS) applications. The simulated and measured results verify the null steering performance of the proposed design.**

***Index Terms*—Circularly polarized antennas, global positioning system antennas, null steering.**

I. Introduction

CIRCULARLY POLARIZED (CP) patch antennas are widely used in the global position system (GPS) applications. To track as many satellites as possible, broad beam coverage in the upper hemisphere is required. However, wide angle coverage is vulnerable to intentional electromagnetic jamming. Therefore, the null steering antenna (NSA) is developed to suppress the interference signal. By reconfiguring the radiation pattern, NSA can generate a null towards a specific direction where the interference source is placed. A common NSA approach is to use phased array antennas [1][2]. The feeding weight of each antenna element can be changed and optimized to generate a steerable null. Another proposal is to use parasitic array antennas to reduce the number of phase shifters [3].

Pattern reconfigurable/diversity antennas provide another approach of null steering without large physical dimensions. For example, p-i-n diodes [4] and varactors [5][6] are adopted to achieve a discrete or continuous null steering. However, the null steering method is for linearly polarized (LP) wave. Recently, pattern diversity antennas with multiple modes have been proposed to achieve null steering. Broadside and omnidirectional (conical) pattern modes are the typical pair of modes. The synthetic radiation of the two modes can be tuned to generate a null at the specific direction. According to the polarization of the two modes, various design types have been proposed [7]–[11]. For example, the broadside and conical pattern modes in [7] are synthesized to achieve a two-dimensional (2-D) LP null steering in the elevation plane. In [8], a dielectric resonator antenna (DRA) is excited by one port for the conical pattern mode, and a patch antenna is added and excited by two ports for the broadside pattern mode. Three-dimensional (3-D) LP null steering is achieved by adjusting the power ratio of the three feeding ports. In [9], another 3-D LP null steering antenna is proposed. A monopole and a corner-truncated patch are combined and fed by two ports. By tuning the power ratio and phase difference of the two ports, the null is steerable in the elevation and azimuth planes. In [10], a broadside CP pattern and a conical LP pattern are excited on the same rectangular patch. A null is generated and steerable in the low elevation angles. In [11], the TM_{11} and TM_{21} modes of two microstrip antennas are excited for broadside CP pattern and conical CP pattern. 3-D null steering is achieved in the upper hemisphere. However, the use of TM_{21} mode leads to large antenna size and the use of hybrid couplers leads to a complex feeding network.

In this letter, a novel CP antenna with conical and broadside modes is proposed and measured for 3-D null steering. Four rotationally symmetric strips, which are first described in [12], are fed in phase to excite the conical mode. A corner-truncated patch is used to excite the broadside mode and achieve wide 3-dB axial ratio (AR) beamwidth. The null is produced and controlled by changing the exciting power ratio and exciting phase delay of the two modes. By controlling the exciting power ratio of the two modes, continuous null steering is achieved in the upper elevation plane. By controlling the phase delay of the two modes, continuous null steering is achieved in the whole azimuth plane. The proposed NSA shows potential use in the anti-interference of GPS applications.

II. Antenna Design

Fig. 1 shows the geometry of the proposed antenna. The assembled antenna consists of two FR4 ($\varepsilon_r = 4.4, \tan\delta = 0.02$) substrate layers. The thickness of the upper substrate (#1) and the lower substrate (#2) is 0.8 mm and 2 mm, respectively. The air gap between the two substrate layers has a thickness of 10.2 mm. The two substrate layers are assembled together

Manuscript received September 24, 2014; revised December 07, 2014; accepted December 10, 2014. Date of publication December 18, 2014; date of current version March 19, 2015. This work was supported by the National Basic Research Program of China under Contract 2013CB329002 , in part by the National Natural Science Foundation of China under Contract 61301001 , the National Science and Technology Major Project of the Ministry of Science and Technology of China 2013ZX03003008-002 , the China Postdoctoral Science Foundation funded project 2013M530046 , the Beijing Excellent Doctoral Dissertation Instructor project 20131000307 .

The authors are with the State Key Laboratory on Microwave and Digital Communications, Tsinghua National Laboratory for Information Science and Technology, Department of Electronic Engineering, Tsinghua University, Beijing, China (e-mail: dengcj11@gmail.com; lyee@tsinghua.edu.cn).

Color versions of one or more of the figures in this letter are available online at http://ieeexplore.ieee.org.

Digital Object Identifier 10.1109/LAWP.2014.2382107

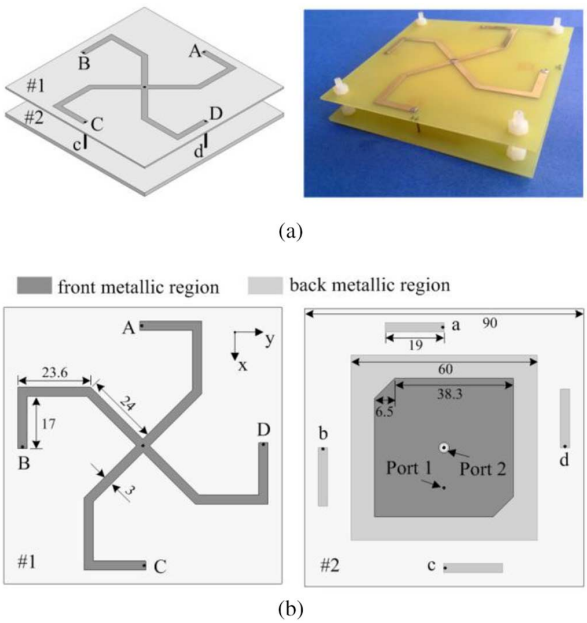

Fig. 1. Configuration of the proposed antenna. (a) 3-D view. (b) Transparent view of each substrate layer and detailed dimensions (Unit: mm).

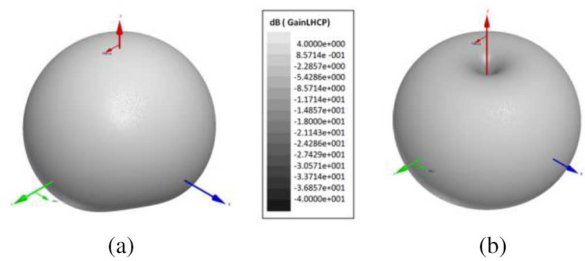

Fig. 2. Simulated 3D radiation pattern. (a) Fed by Port 1. (b) Fed by Port 2.

by five metallic pins, namely A-a, B-b, C-c, D-d, and the central-placed pin, as shown in Fig. 1(a). Fig. 1(b) shows the transparent view of the upper and lower substrate layers. On the front of the upper substrate, four rotationally symmetric metallic strips are joined together at the centre. These four strips are connected with their corresponding strips on the back of the lower substrate via four pins (A-a, B-b, C-c, D-d), and are fed by Port 2 via the central-placed pin. A corner-truncated patch is printed on the front of the lower substrate layer, and is fed by Port 1. High Frequency Structure Simulator (HFSS) is used to optimize the dimensions of the proposed antenna.

The broadside CP pattern mode is generated by a traditional corner-truncated patch antenna, as is shown in Fig 2(a). Thick substrate thickness is utilized to obtain broad beam coverage. Fig. 3 shows the simulated AR distribution at 1.575 GHz when only Port 1 is excited. It is shown that the AR gets worse with the increase of the elevation angle, θ. The 3-dB AR criterion is satisfied from $\theta = 0°$ to about $\theta = 50°$.

The conical CP pattern mode is generated by the four folded strips, as is shown in Fig 2(b). The operating mechanism of circular polarization for the conical mode is studied in [12], where the four strips are viewed as four tilted and crossed elements. The horizontal strips and vertical pins of the four elements correspond to the two electric field components ($E\varphi$ and E_θ) for

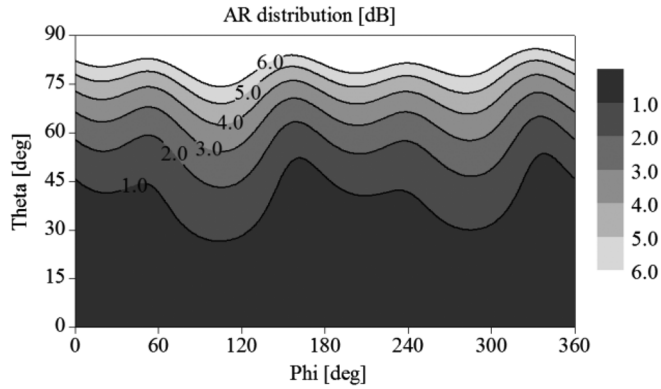

Fig. 3. Simulated AR distribution for broadside pattern at 1.575 GHz.

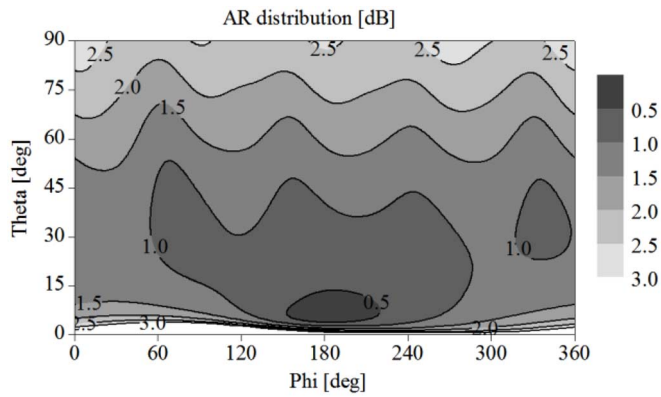

Fig. 4. Simulated AR distribution for conical pattern at 1.575 GHz.

circular polarization. Thus, $E\varphi$ can be optimized by tuning the strips on the back of the lower substrate. Fig. 4 shows the AR distribution at 1.575 GHz when only Port 2 is excited. It is observed that the AR is less than 3 dB in most of the upper hemisphere, except around the zenith. From $\theta = 0°$ to about $\theta = 70°$, the AR is less than 2 dB. In addition, the AR variation in the azimuth plane is less than 1 dB.

III. Experimental Results

Fig. 5 shows the simulated and measured S parameters. It is observed that the measured results have a slight shift towards the higher frequency. This difference is mainly caused by the uncertain permittivity of substrate. The measured overlapping -10-dB impedance bandwidth for both modes fed through Port 1 and Port 2 is 87 MHz (1.558-1.645 GHz). The measured port isolation is about -30 dB over the entire bandwidth. Since the measured results have a slight frequency shift, the simulated patterns and ARs are chosen at 1.575 GHz, while the measured results are chosen at 1.6 GHz.

As mentioned in Section I, radiation null can be synthesized from the broadside and the omnidirectional pattern modes. The theoretical null analysis for linear polarization is systematically studied in [9]. A null for circular polarization with infinite negative value can be achieved under the condition discussed in [9] and the condition AR $= 0$ dB. However, for practical use, the AR performance will deteriorate a little bit due to the operating environment and fabrication error. Therefore, we will check our idea of reconfigurable null steering using the practical measured

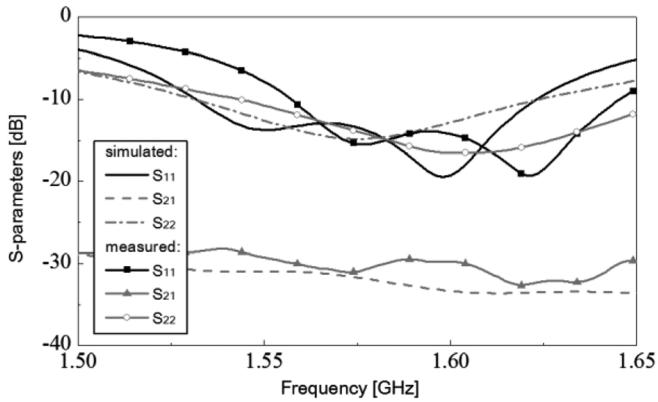

Fig. 5. Simulated and measured S parameters of the proposed antenna.

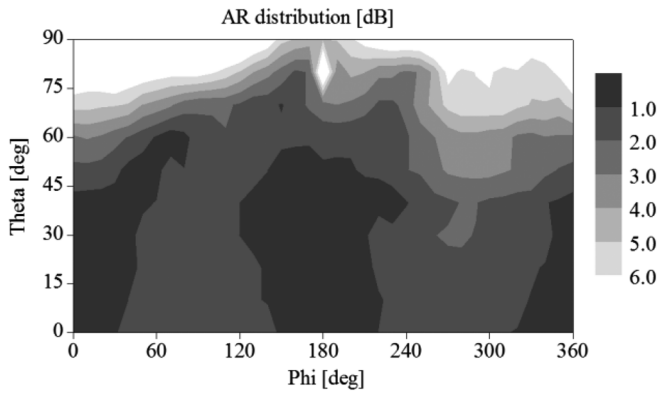

Fig. 6. Measured AR distribution for broadside pattern at 1.6 GHz.

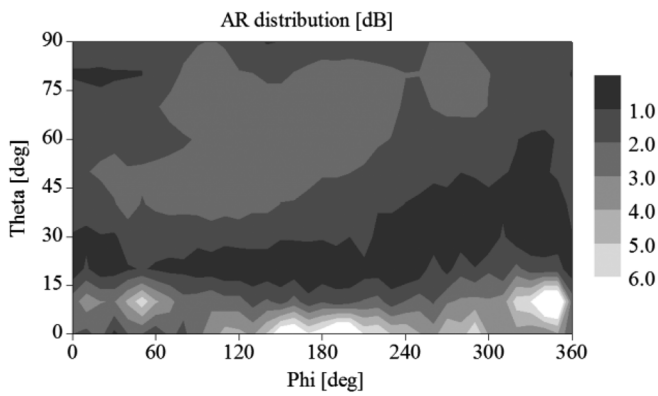

Fig. 7. Measured AR distribution for conical pattern at 1.6 GHz.

field results. Based on the measured AR distributions of the two modes illustrated in Fig. 6 and 7, the postprocessing on the radiation patterns of the two modes for 3-D null steering will be discussed in detail. It is worth mentioning that the measured AR at $\theta = 0^\circ$ is not constant, owing to the method error in [13].

The exciting power ratio and relative phase delay of Port 1 and Port 2 are the two key factors for 3-D CP null steering. To be specific, by changing the exciting power ratio, the pattern null is steerable in the elevation plane; by changing the relative phase delay, the pattern null is steerable in the azimuth plane. The control of exciting power ratio and phase delay of the two ports is

TABLE I
SIMULATED NULL STEERING IN THE ELEVATION PLANE AT 1.575 GHZ

parameter A	16	8	4	2	1	0.5	0.25
null angle (°)	12	18	24	34	48	62	75
null depth (dB)	28.4	25.8	23.9	23.5	23.1	20.6	17.4

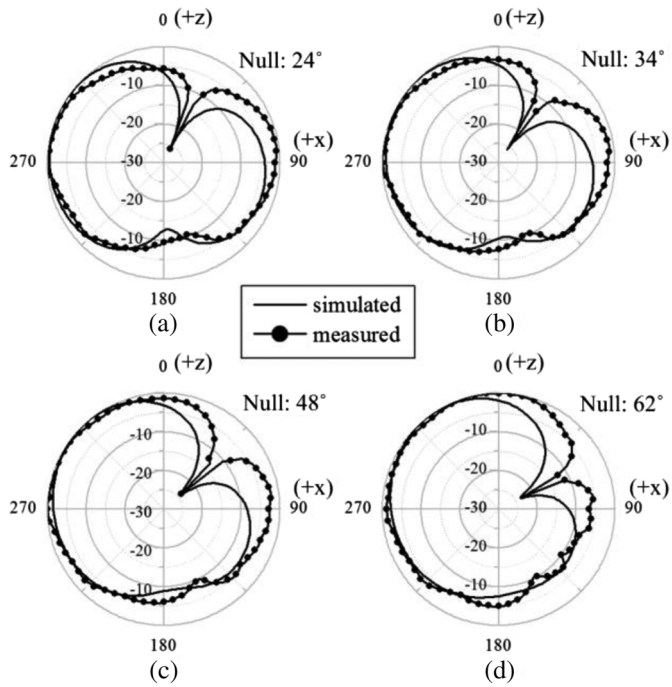

Fig. 8. Simulated and measured normalized synthetic radiation patterns with null at different elevation angles.

easy in HFSS software, and the simulated synthetic radiation pattern can also be derived directly. The measured synthetic radiation pattern is derived from the measured results according to the following steps:

- measure the radiation patterns with magnitude and phase for broadside and conical pattern modes, separately
- import and format the radiation patterns for Port 1 (E_b) and Port 2 (E_o) with MATLAB tool
- calculate the synthetic pattern ($E_{\rm tot}$) using $E_{\rm tot} = E_b + {\rm A}{\cdot}{\rm e}^{{\rm j}{\rm B}} \cdot E_o$

where A is the factor of exciting power ratio, B is the relative phase delay.

The null steering in the elevation plane will be discussed first. In this case, parameter B is fixed at 0°, corresponding to the $\varphi = 0$ plane. Table I shows the simulated null steering in the elevation plane. It is observed that with the decease of parameter A, the null angle increases, while the null depth decreases. This is because the AR of the broadside mode gets worse when the elevation angle increases. A further discussion is made in Fig. 8, where the simulated results (at 1.575 GHz) and the measured results (at 1.6 GHz) are shown. The detailed configuration of A and B is listed in Table II. It is shown that the null depth at all the null elevation angles is above 20 dB. Considering fabrication and measurement errors, parameter B (the relative phase delay) for measurement is also fine-tuned to get a deep null. Therefore,

TABLE II
CONFIGURATION FOR NULL STEERING IN THE ELEVATION PLANE

		(a)	(b)	(c)	(d)
Simulation	A	4	2	1	0.5
	B	0°	0°	0°	0°
Measurement	A	3.67	1.88	1.09	0.53
	B	-2°	-1°	-14°	-16°

TABLE III
SIMULATED NULL STEERING IN THE AZIMUTH PLANE AT 1.575 GHZ

parameter B (°)	0	45	90	135	180	225	270	315
null angle (°)	0	45	90	135	180	225	270	315
null depth (dB)	24.3	26.3	22.9	21.4	24.3	26.1	21.7	21.0

TABLE IV
CONFIGURATION FOR NULL STEERING IN THE AZIMUTH PLANE

		(a)	(b)	(c)	(d)
Simulation	A	1	1	1	1
	B	45°	135°	180°	225°
Measurement	A	0.86	0.93	1.09	1.03
	B	48°	142°	166°	219°

the null is steerable in the elevation plane by controlling the exciting power ratio.

For the null steering in the azimuth plane, parameter A is fixed at 1, corresponding to the $\theta = 48°$ plane. Table III shows the simulated null steering in the azimuth plane. It is observed that the variation of parameter B causes an equal change of the null angle. The null depth varies but is above 20 dB in all cases. A further discussion is made in Fig. 9, where the simulated results (at 1.575 GHz) and the measured results (at 1.6 GHz) are shown. The detailed configuration of A and B is listed in Table IV. Deep null depth (above 20 dB) is achieved at all the null azimuth angles. Similarly, parameter A (the exciting power ratio) for measurement is also fine-tuned for null depth optimization. Therefore, the null is steerable in the azimuth plane by controlling the relative phase delay. Three-dimensional null steering can be achieved by properly controlling the exciting power ratio and relative phase delay of the two ports.

IV. CONCLUSION

In this letter, a compact 3-D CP null steering antenna is proposed. The design of the broadside and the conical CP pattern modes is discussed in detail. The measured overlapping bandwidth for Port 1 and Port 2 with 10-dB return loss and 3-dB AR criterion is about 22 MHz. The simulated and the measured results show that by controlling the port power ratio and the relative phase delay of the two feeding ports, the synthetic pattern null is steerable in the upper hemisphere. With the merit of reconfigurable null, the proposed CP antenna is suitable for the anti-interference of GPS applications.

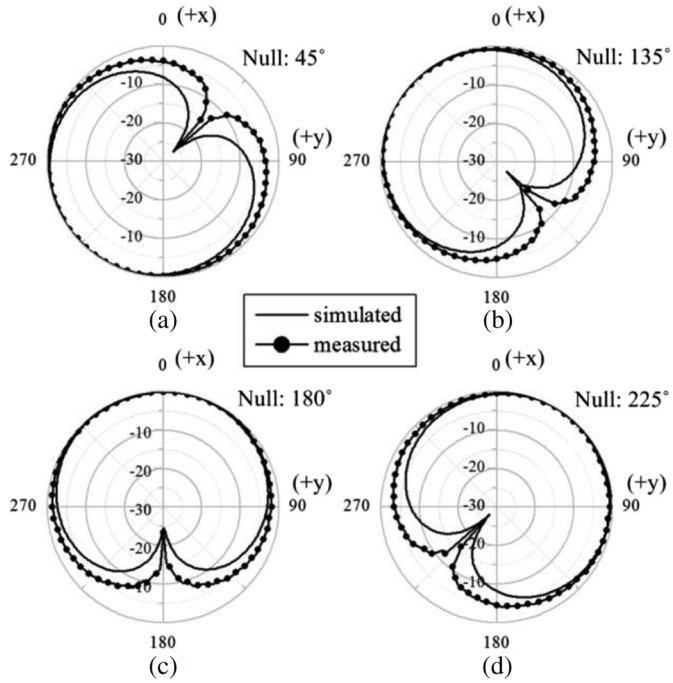

Fig. 9. Simulated and measured normalized synthetic radiation patterns with null at different azimuth angles.

REFERENCES

[1] C. Ko, "A fast null steering algorithm for linearly constrained adaptive arrays," *IEEE Trans. Antennas Propag.*, vol. 39, no. 8, pp. 1098–1104, Aug. 1991.
[2] T. Vu, "On null steering in rectangular planar array," *IEEE Trans. Antennas Propag.*, vol. 40, no. 8, pp. 995–997, Aug. 1992.
[3] C. Sun, A. Hirata, T. Ohira, and N. C. Karmakar, "Fast beamforming of electronically steerable parasitic array radiator antennas: Theory and experiment," *IEEE Trans. Antennas Propag.*, vol. 52, no. 7, pp. 1819–1832, Jul. 2004.
[4] M. Parihar, A. Basu, and S. Koul, "Efficient spurious rejection and null steering using slot antennas," *IEEE Antennas Wireless Propag. Lett.*, vol. 10, pp. 207–210, 2011.
[5] S. Yong and J. T. Bernhard, "Reconfigurable null scanning antenna with three dimensional null steer," *IEEE Trans. Antennas Propag.*, vol. 61, no. 3, pp. 1063–1070, Mar. 2013.
[6] S. Yong and J. T. Bernhard, "A pattern reconfigurable null scanning antenna," *IEEE Trans. Antennas Propag.*, vol. 60, no. 10, pp. 4538–4544, Oct. 2012.
[7] X. Jiang, Z. Zhang, Y. Li, and Z. Feng, "A novel null scanning antenna using even and odd modes of a shorted patch," *IEEE Trans. Antennas Propag.*, vol. 62, no. 4, pp. 1903–1909, Apr. 2014.
[8] N. R. Labadie, S. K. Sharma, and G. Rebeiz, "Multimode antenna element with hemispherical beam peak and null steering," in *Proc. IEEE AP-S Int. Symp. Antennas Propag.*, 2012, pp. 1–2.
[9] Y. Li, Z. Zhang, C. Deng, and Z. Feng, "A simplified hemispherical 2-D angular space null steering approach for linearly polarization," *IEEE Antennas Wireless Propag. Lett.* vol. 13, pp. 1628–1631, 2014.
[10] M. N. Solomon, "Multimode rectangular microstrip antenna for GPS applications," in *Proc. IEEE AP-S Conf. Antennas Propag. Wireless Commun.*, 1998, pp. 149–151.
[11] N. R. Labadie, S. K. Sharma, and G. M. Rebeiz, "A circularly polarized multiple radiating mode microstrip antenna for satellite receive applications," *IEEE Trans. Antennas Propag.*, vol. 62, no. 7, pp. 3490–3500, Jul. 2014.
[12] C. Deng, Y. Li, Z. Zhang, and Z. Feng, "A circularly polarized pattern diversity antenna for hemispherical coverage," *IEEE Trans. Antennas Propag.*, vol. 62, no. 10, pp. 5365–5369, Oct. 2014.
[13] A. B. Constantine, *Antenna Theory: Analysis and Design*. New York, NY, USA: Wiley-Interscience, 2005, pp. 73–74.